Biology of Reproduction, 2023, **108(5)**, 802–813
https://doi.org/10.1093/biolre/ioad019
Advance access publication date 15 February 2023
Research Article

Presence of ovarian stromal aberrations after cessation of testosterone therapy in a transgender mouse model†

Hadrian M. Kinnear[1,2], Prianka H. Hashim[3], Cynthia Dela Cruz[3], Alexis L. Chang[4], Gillian Rubenstein[5], Likitha Nimmagadda[4], Venkateswaran Ramamoorthi Elangovan[6], Andrea Jones[4], Margaret A. Brunette[4], D. Ford Hannum[7], Jun Z. Li[7], Vasantha Padmanabhan[3,6], Molly B. Moravek[3,8,9] and Ariella Shikanov[1,3,4,*]

[1]Program in Cellular and Molecular Biology, University of Michigan, Ann Arbor, MI, USA
[2]Medical Scientist Training Program, University of Michigan, Ann Arbor, MI, USA
[3]Department of Obstetrics and Gynecology, University of Michigan, Ann Arbor, MI, USA
[4]Department of Biomedical Engineering, University of Michigan, Ann Arbor, MI, USA
[5]Women's and Gender Studies Department, University of Michigan, Ann Arbor, MI, USA
[6]Department of Pediatrics and Communicable Diseases, University of Michigan, Ann Arbor, MI, USA
[7]Department of Computational Medicine and Bioinformatics, University of Michigan, Ann Arbor, MI, USA
[8]Division of Reproductive Endocrinology and Infertility, University of Michigan, Ann Arbor, MI, USA
[9]Department of Urology, University of Michigan, Ann Arbor, MI, USA

*__Correspondence__: Department of Biomedical Engineering, University of Michigan, 1101 Beal Ave, 2126 LBME, Ann Arbor, MI 48109, USA.
E-mail: shikanov@umich.edu

†__Grant support__: This work was supported by the National Institutes of Health grant R01-HD098233 to MBM, the American Society for Reproductive Medicine / Society for Reproductive Endocrinology and Infertility Grant to MBM, and University of Michigan Office of Research funding U058227 to AS. Effort of HMK was supported by the National Institutes of Health grants F30-HD100163 and T32-HD079342. Effort of CDC was supported by the Michigan Institute for Clinical and Health Research grants KL2 TR 002241 and UL1 TR 002240. The University of Virginia Center for Research in Reproduction Ligand Assay and Analysis Core was supported by the Eunice Kennedy Shriver National Institute of Child Health and Human Development grants P50-HD028934 and R24-HD102061.

Abstract

Some transmasculine individuals may be interested in pausing gender-affirming testosterone therapy and carrying a pregnancy. The ovarian impact of taking and pausing testosterone is not completely understood. The objective of this study was to utilize a mouse model mimicking transmasculine testosterone therapy to characterize the ovarian dynamics following testosterone cessation. We injected postpubertal 9–10-week-old female C57BL/6N mice once weekly with 0.9 mg of testosterone enanthate or a vehicle control for 6 weeks. All testosterone-treated mice stopped cycling and demonstrated persistent diestrus within 1 week of starting testosterone, while control mice cycled regularly. After 6 weeks of testosterone therapy, one group of testosterone-treated mice and age-matched vehicle-treated diestrus controls were sacrificed. Another group of testosterone-treated mice were maintained after stopping testosterone therapy and were sacrificed in diestrus four cycles after the resumption of cyclicity along with age-matched vehicle-treated controls. Ovarian histological analysis revealed stromal changes with clusters of large round cells in the post testosterone group as compared to both age-matched controls and mice at 6 weeks on testosterone. These clusters exhibited periodic acid–Schiff staining, which has been previously reported in multinucleated macrophages in aging mouse ovaries. Notably, many of these cells also demonstrated positive staining for macrophage markers CD68 and CD11b. Ovarian ribonucleic acid-sequencing found upregulation of immune pathways post testosterone as compared to age-matched controls and ovaries at 6 weeks on testosterone. Although functional significance remains unknown, further attention to the ovarian stroma may be relevant for transmasculine people interested in pausing testosterone to carry a pregnancy.

Summary Sentence
After testosterone is paused for reproductive purposes in a transgender mouse model, estrous cyclicity resumes, but ovaries demonstrate stromal aberrations and an upregulated inflammatory reaction.

Received: November 7, 2022. **Revised:** January 25, 2023. **Accepted:** February 10, 2023

Graphical Abstract

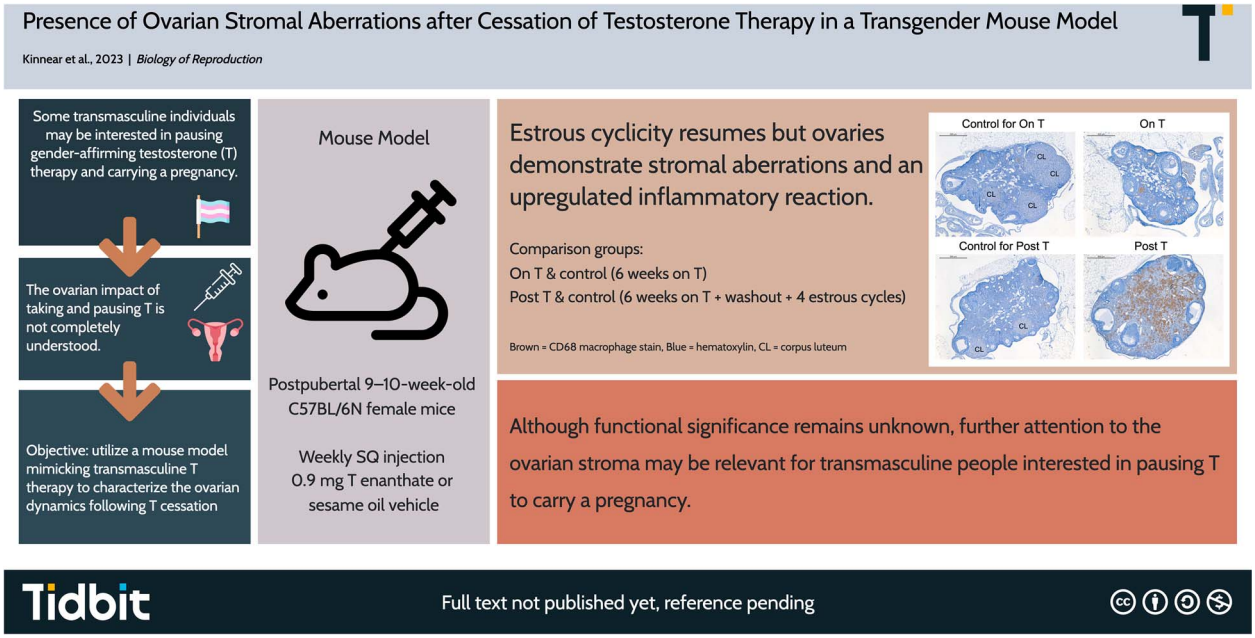

Key words: mouse, ovary, testosterone, transgender, stroma, immune, macrophage

Introduction

Transmasculine individuals may utilize gender-affirming testosterone (T) therapy, typically via intramuscular or subcutaneous injections or via transdermal applications [1]. Although current clinical guidelines encourage discussion of fertility preservation prior to starting T therapy [1–3], emerging literature points to the possibility of transmasculine individuals being able to use their gametes for reproduction after being on T [4–13]. Some transmasculine individuals have utilized oocyte retrieval to allow a partner or surrogate to carry a pregnancy with their gametes [6, 8, 9, 12], while others have carried a pregnancy themselves after being on T [4, 5, 7, 8, 10, 11]. Notably, multiple transmasculine individuals have reported intentionally stopping T in order to become pregnant, including 17 individuals in a survey by Light et al., 2014 and 5 individuals in a survey by Moseson et al., 2021 [4, 10]. Surveys of future intent also provide support to the premise that some transmasculine individuals might pause T to carry a pregnancy. Light et al., 2018 surveyed 18–45-year-old transmasculine individuals (197 total, 86% with prior or current T use) to better understand contraceptive practices and fertility desires and found that a quarter were interested in carrying a pregnancy themselves [7]. Moseson et al., 2021 surveyed 1694 transgender, nonbinary, and gender-expansive individuals assigned female or intersex at birth and found that 11% were interested in a future pregnancy and 16% were not sure [10]. As transmasculine individuals may be interested in pausing T to carry a pregnancy, it is important to gain a clear understanding of the impact on the ovary of taking and pausing T. Although several studies have reported transmasculine pregnancies after varied durations of T therapy, these studies often selected for individuals with successful pregnancies and so do not provide information about potential others who may have had difficulty conceiving or carrying to term [4, 5, 11]. A better understanding of ovarian dynamics during T therapy and after T cessation is needed to provide relevant reproductive information to transmasculine individuals considering pausing T to pursue pregnancy.

Available evidence from transmasculine individuals points to the impact of T therapy on cyclicity, follicular distribution, and corpora lutea formation. Specifically, T therapy has been shown to suppress menstrual cycles, potentially via negative feedback at neural and pituitary levels [14], increase cystic or atretic follicles, and reduce or block corpora lutea formation [15]. Encouragingly, a relatively normal cortical distribution of primordial to primary follicles has been reported from analyses of human ovaries on T [16]. We have developed a mouse model mimicking transmasculine T therapy that yielded similar outcomes, namely acyclicity with increased numbers of atretic large antral follicles and no corpora lutea in C57BL/6N mice at 6 weeks on T, with no detectable loss in primordial follicles as compared to controls [17]. Subsequent studies by Bartels et al. revealed a reduction in corpora lutea and no detectable differences in antral or atretic antral follicles following 6 weeks of T injections in CF-1 mice [18]. Encouragingly, their mice produced fertilizable eggs with superovulation on T [18]. Bartels et al. noted that their approach matches a clinical situation where the transmasculine individual does not plan to carry the pregnancy themselves at that time [18]. In this setting, ovarian support for pregnancy including corpora lutea formation is not needed, and accordingly, they do not report a thorough ovarian histological comparison after T washout [18]. For transmasculine individuals interested in carrying a pregnancy, T therapy should be paused, and it is important to consider both follicular development and corpora lutea formation after T cessation and washout. More recently, in a study focused

on resumption of cyclicity, we noted that after T implants were removed at 6 weeks, C57BL/6N mice promptly started to cycle within a week and ovaries formed corpora lutea after four estrous cycles [19]. Beyond our previous study, there is limited literature looking at cyclicity, follicular distribution, and corpora lutea formation if T is paused for reproductive purposes.

Notable T-induced changes to the ovarian stroma have also been reported for transmasculine individuals. These include increased collagenization of the tunica albuginea or outer cortex [20–23], stromal hyperplasia [20–24], and luteinization of stromal cells [20–23], which are characteristics also frequently observed in polycystic ovary syndrome [25]. There has been minimal investigation of this stromal hyperplasia or luteinization beyond descriptive observations. Recent reports have demonstrated similar stromal changes in mouse models of polycystic ovary syndrome induced with dihydrotestosterone (DHT) [26, 27]. Candelaria et al., 2019 found clusters in the ovarian stroma of hyperplastic and lipid-filled cells after 2 months of DHT treatment starting at postnatal day 25 [26]. Similarly, Sun et al., 2019 observed a DHT-induced hypertrophic lipid-filled stroma after 60 days of DHT treatment starting at postnatal day 25 [27]. Cellular characterization of prolonged T- or DHT-induced changes to the ovarian stroma has been challenging, in part due to the fact that many of the cell types of the ovarian stroma are not well understood [28].

Investigating ovarian changes if T is paused for reproductive purposes is logistically difficult in human patients. Mouse models mimicking gender-affirming T therapy can provide direction to help to fill this gap. We previously reported that the drop in T levels after removal of T implants correlated with resumption of estrous cyclicity and noted typical follicular distributions after four estrous cycles [19]. As gender-affirming T therapy is frequently injection-based, the objective of this study was to utilize an injection-based mouse model mimicking transmasculine T therapy to characterize the ovarian dynamics if T is paused for reproductive purposes. Unexpectedly, this study design allowed us to capture ovaries after T cessation in the midst of notable stromal changes and to subsequently probe more deeply into this unusual stromal state.

Materials and methods

Ethical approval

All animal work was conducted in compliance with a protocol approved by the University of Michigan Institutional Animal Care & Use Committee (PRO00007618, PRO00009635).

Experimental design

This study used 40 C57BL/6NHsd female mice (Envigo, Indiana, IN, USA). Mice were housed in groups of five in ventilated cages and had free access to food and water and a 12-h light/dark cycle within a non-barrier facility at the University of Michigan. Mice started T therapy at 9–10 weeks old (body mass 18.7 ± 0.7, mean $\pm$ SD). Controls received a sesame oil only injection. T therapy was administered via a weekly (Thurs PM) subcutaneous mid-back injection (100 μL). Each dose included 0.9 mg T enanthate, diluted with sesame oil from a 200 mg/mL stock (Hikma Pharmaceuticals, Portugal). Further details on T injection dose selection are included in our recently published T pharmacokinetic comparison, which compares weekly T levels with different dosing paradigms and includes mice from this study [29]. Sesame oil was sterile filtered before use (USP/NF grade, Welch, Holme & Clark Co., Inc., Newark, NJ, USA). All T-treated mice ($n = 20$) were treated with T for 6 weeks. At 6 weeks on T, one cohort was sacrificed ("On T," $n = 10$) and compared to parallel age-matched controls ("Control for On T" or "Control OT," $n = 10$). In a separate cohort, T was stopped after 6 weeks and allowed to washout. These mice were followed until resumption of estrous cyclicity and sacrificed after four estrous cycles ("Post-T," $n = 10$), with parallel age-matched controls ("Control for Post-T" or "Control PT," $n = 10$). All mice were sacrificed in diestrus and ovaries were collected for further analysis.

Vaginal cytology

Vaginal cytology was collected daily starting 2–3 weeks prior to the first T injection and continuing until sacrifice. The distribution of leukocytes, cornified epithelial cells, and nucleated epithelial cells was evaluated to determine estrous cycle stage.

Blood collection and hormone analysis

Blood for T analysis was collected from the lateral tail vein at volumes not exceeding 0.5% of the bodyweight at the midpoint between doses (Mon AM). Terminal blood collection was performed via cardiac puncture under isoflurane anesthesia. After overnight storage at 4°C, blood samples were centrifuged for 10 min ($\leq$8100G) and serum was collected and stored until analysis at −20°C. Hormone analyses were performed by the Ligand Assay and Analysis Core Facility at the University of Virginia Center for Research in Reproduction. The reportable range for a coefficient of variance <20% for the Testosterone Mouse and Rat enzyme-linked immunosorbent assay was 0.10–16 ng/mL or 0.20–32 ng/mL with a 2x dilution (Immuno-Biological Laboratories, Inc.; IB79106, Minneapolis, MN, USA, RRID:AB_2814981).

Ovarian histological and follicular distribution analyses

Mouse ovaries within perigonadal fat (one per mouse) were fixed overnight at 4°C in the Bouin fixative ($n = 5$/group) or 4% paraformaldehyde ($n = 5$/group), paraffin-embedded at the University of Michigan School of Dentistry Histology Core, serially sectioned (5 μm) with five sections per slide and stained with hematoxylin and eosin (every other slide). All imaging was conducted using a light microscope (DM1000, Leica, Germany). Bouin's-fixed ovaries were used for follicular distribution analyses, corpora lutea counts, and periodic acid–Schiff staining. Paraformaldehyde-fixed ovaries were used for immunohistochemical analyses and corpora lutea counts. Counters were blinded to the experimental group. Primordial, primary, and secondary follicles were counted in every 10th section throughout one entire ovary per mouse at 20–40x magnification. For corpora lutea and antral follicle counts, images at 5x magnification were taken of every 10th section and analyzed alongside each other to prevent overcounting. Primordial follicles were identified by an oocyte with a single squamous granulosa cell layer, primary follicles by an oocyte with a single cuboidal granulosa cell layer, and secondary follicles by an oocyte with two or more granulosa cell layers. To prevent overcounting, we counted primordial

and primary follicles with a visible nucleus and secondary follicles with a visible nucleolus. Discrete round structures with eosinophilic cytoplasm were identified as corpora lutea. Antral follicles were determined by the presence of antral fluid. Atretic late antral follicles were defined as an oocyte lacking connection to granulosa cells and an attenuated granulosa cell layer in a follicle with a well-defined antrum.

Ovarian immunohistochemical analysis and periodic acid–Schiff staining

Ovarian samples fixed in 4% paraformaldehyde, paraffin-embedded, and serially sectioned (5 μm sections, five sections/slide) were used for immunohistochemical analyses. Samples were deparaffinized with xylenes (2 × 10 min), rehydrated in an ethanol series (100/90/70/50/30/0%, 5 min each), treated for 30 min at room temperature with a peroxide block, rinsed in DI water and followed with 20 min of heat-mediated antigen retrieval in 0.1 M sodium citrate buffer pH 6 using a steamer, permeabilized using tris-buffered saline (TBS) with 0.1% Triton X 100 (TBS-T, 2 × 3 min), blocked for 1 h at room temperature in TBS with 10% normal goat serum (NGS), and incubated overnight at 4°C with primary antibody in TBS with 1% NGS. On the following day, samples were washed with TBS-T/TBS (2 × 3 min each), and biotinylated goat anti-rabbit secondary was added for 10 min at room temperature (Abcam rabbit specific HRP/DAB detection IHC kit ab64261, Abcam, Cambridge, UK, RRID:AB_2810213). After a TBS-T/TBS wash (2 × 3 min each), streptavidin peroxidase was added for 10 min at room temperature (ab64261 kit). After another TBS-T/TBS wash (2 × 3 min each), 3,3′-diaminobenzidine was added for 10 min at room temp (ab64261 kit). Samples were then washed with DI water (1 min), counterstained with hematoxylin (2 min with tap water rinse), followed by an ethanol series (30/50/70/90/100%, 5 min each) and xylenes (2 × 10 min) after which samples were mounted with Permount. Additional positive control tissues and secondary-only controls for non-specific staining were utilized. Primary antibodies were used at dilutions in alignment with manufacturer recommendations: Anti-CD68 (rabbit polyclonal, ab125212, Abcam, dilution 1:500, RRID:AB_10975465), Anti-CD11b (rabbit monoclonal, ab133357, Abcam, dilution 1:4000, RRID:AB_2650514), Anti-LHCGR (rabbit polyclonal, bs0984R, Bioss, dilution 1:250, RRID:AB_10859877). A periodic acid–Schiff staining kit (Sigma-Aldrich Inc., St Louis, MO, 395B) was utilized to stain Bouin's fixed ovaries that were paraffin-embedded and serially sectioned (5 μm sections, 5 sections/slide). Slides were deparaffinized in xylenes (2 × 10 min), rehydrated in an ethanol series (100/90/70/50/30/0%, 5 min each), immersed in periodic acid solution for 5 min at room temperature, washed with DI water (3 × 3 min), immersed in the Schiff reagent for 15 min at room temperature, washed in running tap water for 5 min, and counterstained with hematoxylin (90 s with tap water rinse), followed by an ethanol series (30/50/70/90/100%, 5 min each) and xylenes (2 × 10 min) after which samples were mounted with Permount. All samples (n = 3–5 mice/group) were imaged with a light microscope (DM1000, Leica, Germany).

Ovarian ribonucleic acid-sequencing analysis

Mouse ovaries (one per mouse) were micro-dissected from perigonadal fat at the time of sacrifice and stored frozen in ribonucleic acid (RNA) later at −20°C. Tissue disruption and homogenization were performed using the Kimble Biomasher II and QIA shredder homogenizer. The RNA was extracted following manufacturer instructions using the Qiagen RNeasy Mini Kit with Qiagen RNase-Free DNase set and subsequently stored at −80°C. Paired-end RNA-sequencing with poly-A selection was performed by the University of Michigan Advanced Genomics Core on the Illumina NovaSeq 6000 (PE150) using approximately 7.5% of a 300 cycle S4 shared flow cell with 30–40 million reads per sample. Libraries were prepared using the NEBNext Poly(A) mRNA Magnetic Isolation Module (E7490) and NEBNext Ultra II Directional RNA Library Prep Kit for Illumina (E7760) with NEBNext Multiplex Oligos for Illumina (Dual Index Primers Set 2, E7780) (New England Biolabs Inc, Ipswich, MA, USA). Demultiplexed Fastq files were generated with Bcl2fastq2 Conversion Software (Illumina, San Diego, CA, USA). Read mapping and counts were performed by the Advanced Genomics Core. Reads were trimmed using Cutadapt v2.3 [30]; FastQC v0.11.8 [31] was used to ensure data quality and Fastq screen v0.13.0 [32] was used to screen for various types of contamination. Reads were mapped to the reference genome GRCm38 (ENSEMBL) using STAR v2.7.8a [33] and count estimates assigned to genes with RSEM v1.3.3 [34]. Differential expression was analyzed using DESeq2 in R [35]. Gene enrichment was assessed via LRpath using the GO biological process with 50–500 genes, a p-value cutoff of 0.05, and directional analysis for mouse samples identified with Entrez gene IDs [36].

Statistical analysis

GraphPad Prism 9 was used for data analysis. One mouse was the unit of analysis. The Shapiro–Wilk normality test was used to determine parametric and non-parametric testing. The Welch t-test and Brown-Forsythe and Welch one-way analysis of variance with the Dunnett T3 multiple comparisons test were used for parametric testing. Mann–Whitney and Kruskal-Wallis with the Dunn multiple comparisons test were used for non-parametric testing. P-values less than 0.05 were considered statistically significant.

Results

Mice stop cycling during T therapy and resume cycling as T slowly washes out

Within one week of starting T-injections, all T-treated mice stopped cycling and demonstrated persistent diestrus on vaginal cytology (Figure 1, middle). After cessation of T injections at 6 weeks, it took 3.5–10 weeks for mice to resume cycling (Figure 1, middle). All control mice cycled throughout the study (Figure 1, middle). T levels (ng/mL, mean ± SD) were significantly elevated ($P < 0.0001$) in T-treated mice (7.1 ± 1.6) as compared to controls (0.5 ± 0.2) when measured at 6 weeks on T (Figure 1, bottom). T injections were slow to washout, and average T levels were still significantly elevated (0.9 ± 0.3) as compared to controls (0.3 ± 0.1) 7 weeks into the washout period (at week 13) ($P = 0.0016$, Figure 1, bottom). Mice were sacrificed four estrous cycles after resumption of cyclicity, at which point T levels (0.53 ± 0.11) were not significantly different from controls (0.48 ± 0.11, Figure 1, bottom). Cytology traces for all mice included in Supplemental Figure 1.

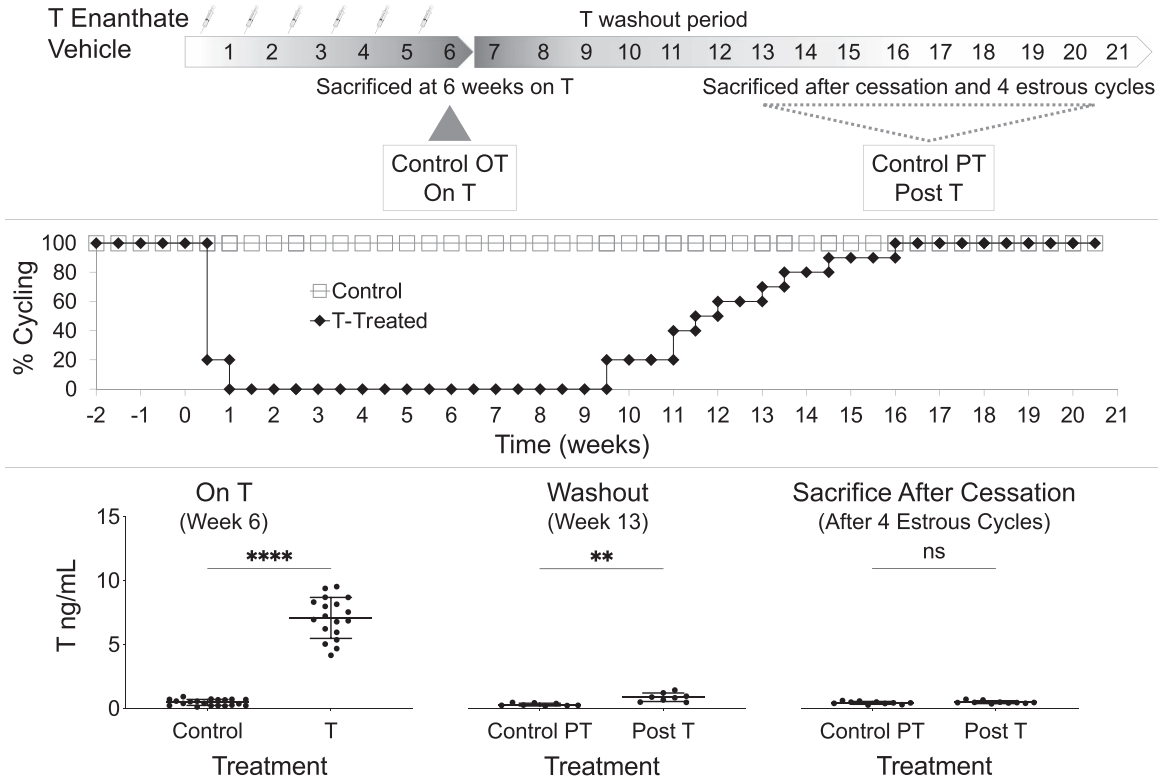

Figure 1. Experimental design, cyclicity, and T levels. (Top) Experimental design of the four study groups: mice sacrificed at 6 weeks on T (On T), parallel age-matched controls for On T (Control OT), mice sacrificed after T cessation and four estrous cycles after resumption of cyclicity (Post-T), and parallel age-matched controls for Post-T (Control PT). (Middle) All T-treated mice stopped cycling within 1 week of starting T and it took 3.5–10 weeks after T cessation at 6 weeks for mice to resume cycling. (Bottom) T levels (ng/mL, mean ± SD) were elevated during T therapy (at 6 weeks on T, $P < 0.0001$), were slow to washout with mean T levels still elevated 7 weeks into the washout period (at week 13, $P = 0.0016$), and were not detectably different from controls when mice were sacrificed four estrous cycles after resumption of cyclicity.

Corpora lutea were absent On T and reduced Post-T with otherwise comparable follicular distributions

Corpora lutea were not observed in ovaries from any mice On T and were only seen for 2 of 10 mice Post-T, with counts (mean ± SD) significantly lower than for control ovaries (Control OT = 6.5 ± 2.1, On T = 0 ± 0, Post-T = 0.7 ± 1.5, Control PT = 9.2 ± 3.0, Figure 2F). Figure 2 displays a representative hematoxylin and eosin-stained ovary (5X) with magnified views of corpora lutea and antral follicles (20X) from each group. No other significant differences were detected in follicle counts (mean ± SD) for primordial follicles (Control OT = 192 ± 67, On T = 255 ± 79, Post-T = 107 ± 55, Control PT = 160 ± 75, Figure 2A), primary follicles (Control OT = 56 ± 20, On T = 40 ± 18, Post-T = 40 ± 14, Control PT = 33 ± 11, Figure 2B), secondary follicles (Control OT = 27 ± 9, On T = 17 ± 4, Post-T = 21 ± 12, Control PT = 21 ± 12, Figure 2C), total antral follicles (Control OT = 25 ± 8, On T = 26 ± 5, Post-T = 27 ± 9, Control PT = 25 ± 4, Figure 2D), or atretic late antral follicles (Control OT = 0.8 ± 1.3, On T = 1.2 ± 1.3, Post-T = 1.0 ± 1.7, Control PT = 0.8 ± 0.8, Figure 2E).

Stromal changes present in ovaries Post-T

Marked ovarian stromal changes were observed in Post-T ovaries, including the presence of large round eosinophilic cells, some of which were in clusters (Figure 3, rows 1 and 2). These changes occurred throughout the stroma of most of the Post-T ovaries. A few similar cells were seen in ovaries from other groups, including Control PT and On T (Figure 3, rows 1 and 2). The stroma in Post-T ovaries also displayed increased clusters of cells that stained intensely with periodic acid–Schiff (Figure 3, rows 3 and 4), which stains polysaccharides, and has been seen in phagocytic cells including ovarian multi-nucleated macrophage giant cells [37].

Notable macrophage-associated staining seen in the ovarian stroma Post-T

Given this increase in periodic acid–Schiff staining, we conducted immunohistochemical staining for two macrophage-associated markers, CD68 and CD11b. Although these stains revealed the presence of macrophages in all ovaries, including some expected macrophage infiltration into the corpus luteum, both CD68 (Figure 4, rows 1 and 2) and CD11b (Figure 4, rows 3 and 4) demonstrated uniquely prominent expression in the large and rounded cells of ovarian stroma Post-T. By contrast, LHCGR staining, which marks luteinized cell types, was not observed in these large round cells in the ovarian stroma Post-T, indicating that these cells are likely not luteinized stromal cells (Figure 4, rows 5 and 6).

Immune pathways upregulated in Post-T as compared to Control PT and On T ovaries

Whole ovary bulk RNA-sequencing ($n = 4$ mice per group, 1 ovary each) demonstrated differences in ovarian gene expression between groups. A heatmap of the top 500 variably expressed genes shows a set of highly upregulated (red) genes

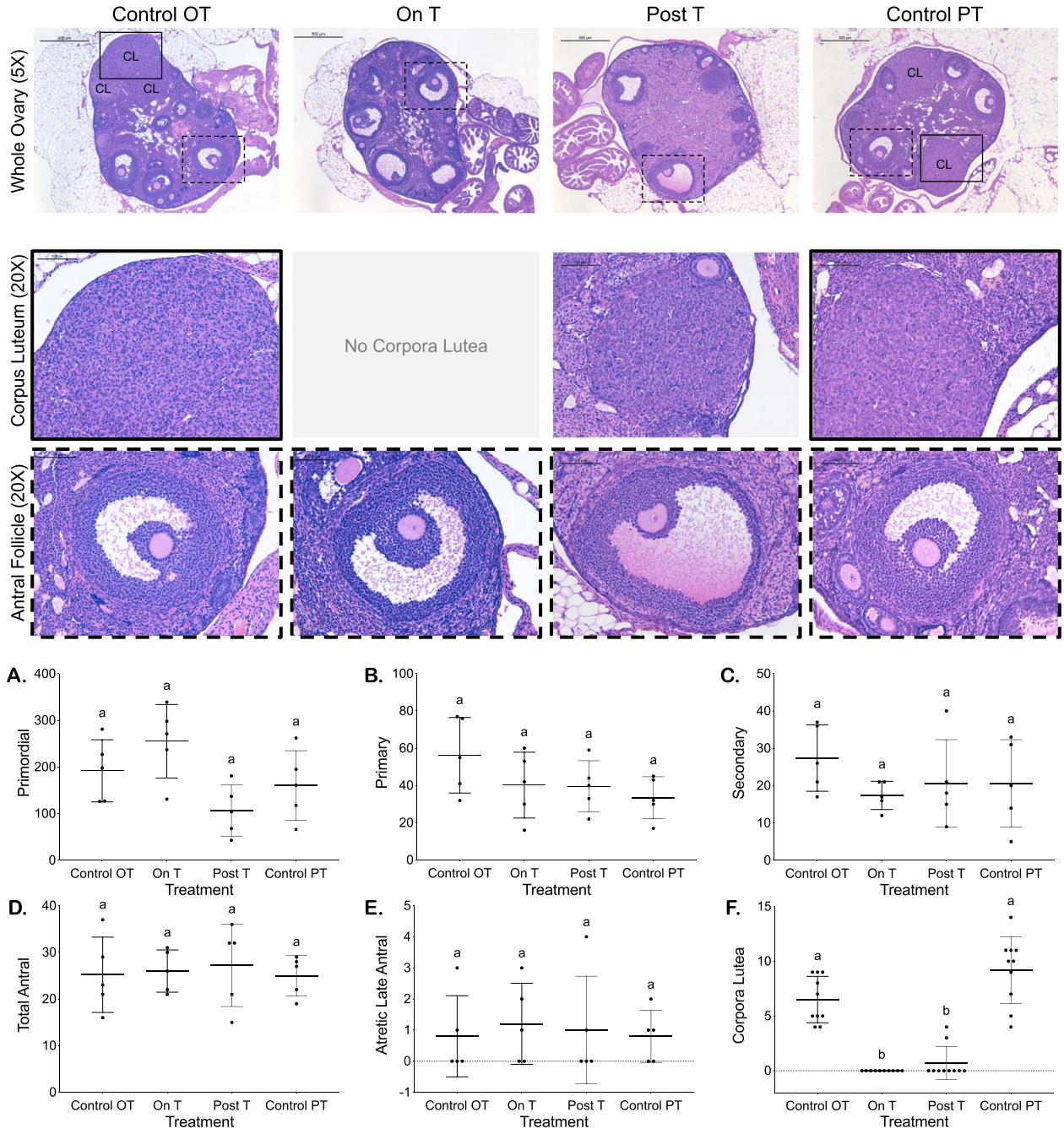

Figure 2. Reduced corpora lutea On T and Post-T with otherwise comparable follicular distributions. Images of hematoxylin and eosin-stained ovaries from all four groups (Control OT, On T, Post-T, and Control PT). Row 1 includes a representative hematoxylin and eosin-stained ovary (5×, scale 500 μm) from each group, while row 2 highlights example corpora lutea (20×, solid outline corresponding to location in 5× image, scale 100 μm), and row 3 highlights example antral follicles (20×, dashed outline corresponding to location in 5× image, scale 100 μm). Follicle counts from every 10th section for primordial (A), primary (B), and secondary (C) follicles. Follicle counts based on 5× images of every 10th section for total antral (D) and atretic late antral (E) follicles as well as corpora lutea (F).

for mice Post-T that are not observed for mice On T or for any of the controls (Figure 5, heatmap top left). Analysis in *LRpath* suggests immune pathway upregulation Post-T when compared to Control PT or On T groups, with the majority of the top 10 gene ontology biological process terms for these comparisons relating to immune system function (e.g., positive regulation of immune response, leukocyte cell–cell adhesion, regulation of cytokine production, regulation of leukocyte activation) (Figure 5, right).

Discussion

Transmasculine individuals may be interested in pausing gender-affirming T to carry a pregnancy, but there are gaps in knowledge regarding the ovarian impact of taking and pausing T. In this study, we utilized a clinically relevant injection-based mouse model mimicking transmasculine T therapy to characterize ovarian dynamics on T and after T cessation. We found a lack of corpora lutea for On T mice, consistent with our prior work [17]. By contrast, we

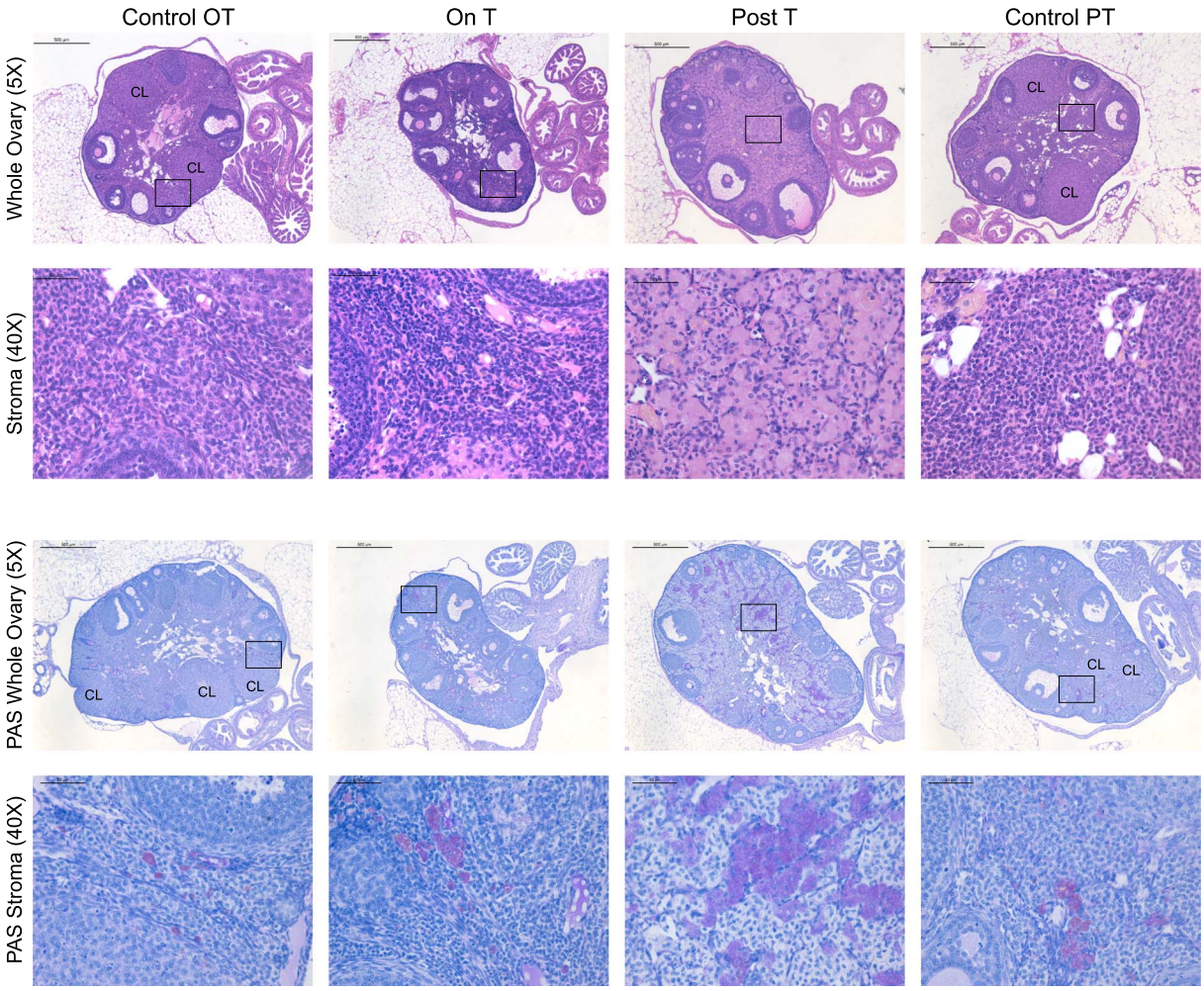

Figure 3. Ovarian stromal changes Post-T. Columns correspond to the four groups: Control OT, On T, Post-T, and Control PT. Row 1 includes a representative hematoxylin and eosin-stained ovary (5×, scale 500 μm) from each group, with the corresponding magnified view of the ovarian stroma in row 2 (40×, scale 50 μm). Row 3 includes a representative magenta periodic acid–Schiff-stained ovary (5×, scale 500 μm) from each group with blue hematoxylin counterstain, with the corresponding magnified view of the ovarian stroma in row 4 (40×, scale 50 μm).

only found corpora lutea for 2/10 Post-T mice, whereas our previous shorter study using T implants for 6 weeks demonstrated corpora lutea in all mice four estrous cycles after T implant removal [19]. Furthermore, we observed unexpected stromal changes in ovaries after T cessation (Post-T) that were not present in parallel age-matched controls (Control PT) or in mice on T for 6 weeks (On T). Of importance, such changes were evident even with resumption of cyclic function. Notably, in our prior study focused on cyclicity after T cessation, we did not observe similarly pronounced stromal changes four cycles after T implant removal at 6 weeks. The key difference between these two studies investigating ovaries approximately four estrous cycles after T cessation was the longer overall T exposure (due to a long T washout) in the current injection-based study, whereas the T exposure in the prior implant-based study was precisely limited to 6 weeks and ceased with removal of the implants [19]. The relevance of these findings is discussed below.

Although we did not evaluate the reproductive function of these mice, the reduction in corpora lutea formation Post-T could potentially lead to difficulties supporting a developing pregnancy. We speculate that there may be a connection between the lack of formation of corpora lutea and the unexpected stromal phenotype, which motivated us to further study the stroma.

Stromal changes evident in Post-T ovaries included an abundance of large round cell clusters. Periodic acid–Schiff stains polysaccharides and strong periodic acid–Schiff staining such as that found in these stromal cell clusters has been previously reported in multinucleated macrophage giant cells present in the ovaries of aging mice [37]. Notably, an abundance of these enlarged ovarian stromal cells in mice Post-T stained positive for CD68 in contrast to age-matched controls (Control PT) and to mice on T for 6 weeks (On T). CD68 is a common macrophage marker, as macrophages highly express CD68 in cell surface, lysosomal, and endosomal membranes [38]. CD68 is also expressed in other cell types, including other mononuclear phagocytes (such as microglia, osteoclasts, and myeloid dendritic cells), with lower levels found in other cell types [38]. Staining for CD11b, a marker of macrophages and other myeloid cells [39], also showed increased expression in the Post-T ovarian stroma. Notably, LHCGR staining was not observed in these stromal cell clusters, suggesting that they likely do not represent a luteinized stromal cell population. In alignment with these observed histologic changes

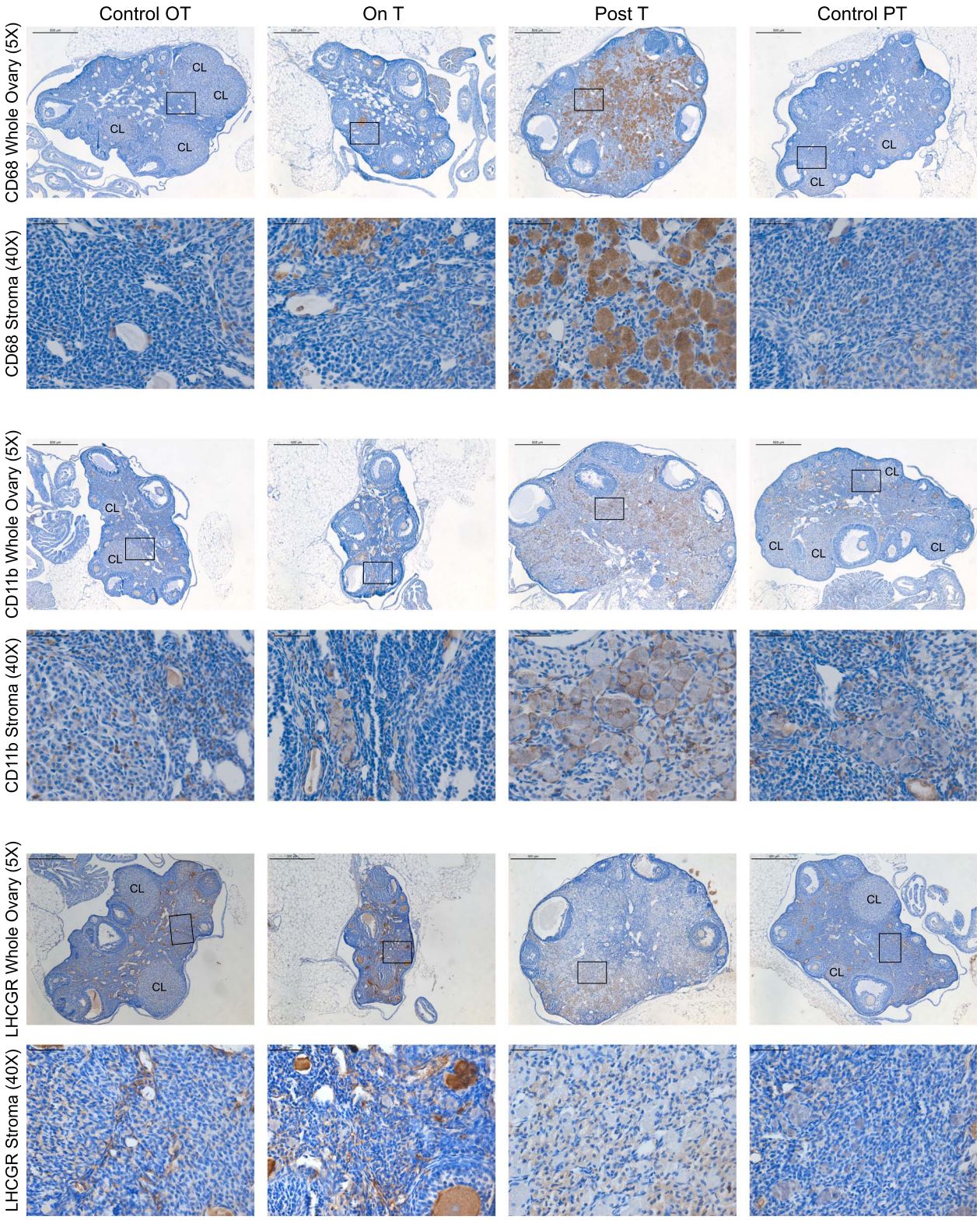

Figure 4. Notable macrophage-associated brown immunohistochemical staining in the ovarian stroma Post-T with blue hematoxylin counterstain. Columns correspond to the four groups: Control OT, On T, Post-T, and Control PT. Row 1 includes representative ovarian CD68 staining (5×, scale 500 μm) from each group, with the corresponding magnified view of the ovarian stroma in row 2 (40×, scale 50 μm). Row 3 includes representative ovarian CD11b staining (5×, scale 500 μm) from each group, with the corresponding magnified view of the ovarian stroma in row 4 (40×, scale 50 μm). Row 5 includes representative ovarian LHCGR staining (5×, scale 500 μm) from each group, with the corresponding magnified view of the ovarian stroma in row 6 (40×, scale 50 μm).

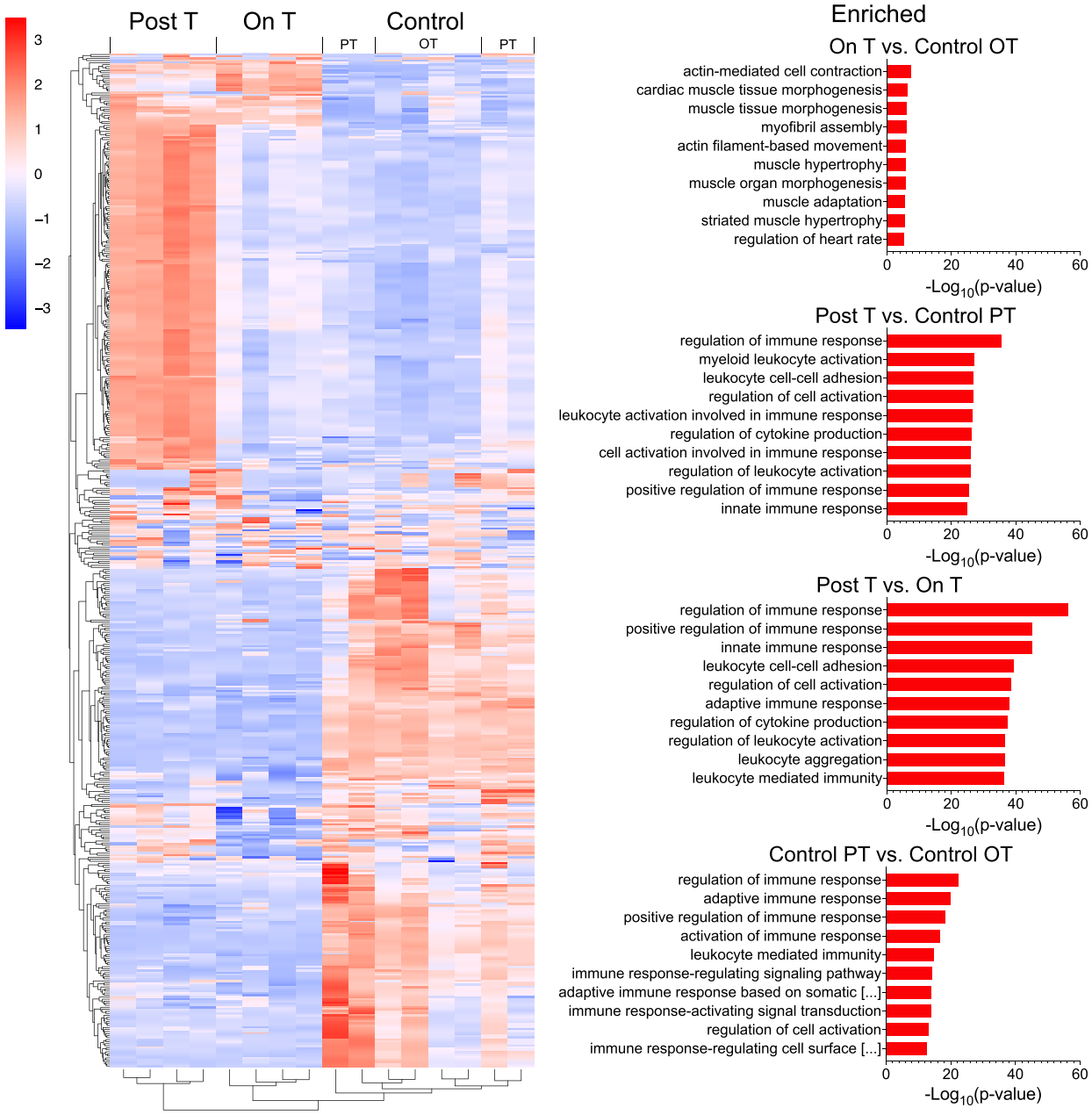

Figure 5. Immune pathway upregulation seen Post-T as compared to Control PT and On T. Heatmap of the top 500 variably expressed genes from whole ovary RNA-sequencing ($n = 4$ mice per group, 1 ovary each). The top 10 gene ontology biological process terms from *LRpath* for genes enriched in the following four comparisons: On T versus Control OT, Post-T versus Control PT, Post-T versus On T, and Control PT versus Control OT. In Control PT versus Control OT, the two titles too long to fully display as shown by [. . .] are: "adaptive immune response based on somatic recombination of immune receptors built from immunoglobulin superfamily domains" and "immune response-regulating cell surface receptor signaling pathway."

representing a stromal immune response with an abundance of macrophages, whole ovary transcriptomic analysis revealed significant upregulation of immune response pathways in Post-T mice as compared to age-matched controls (Control PT) and to mice on T for 6 weeks (On T).

Macrophages are a predominant immune cell type in the ovary and appear to play critical physiologic roles through both phagocytic and secretory functions (reviewed in [40]). They typically are present at low levels in immature or resting ovaries, increase around ovulation near the theca vasculature, and migrate into developing corpora lutea [41]. Ablation of macrophages and other myeloid cells using CD11b-DTR mice led to infertility and hemorrhagic ovaries with impaired corpora lutea [42, 43]. There appear to be multiple subsets of ovarian macrophages and the number, distribution, and function of ovarian macrophages fluctuate over the course of the estrous cycle [39, 44]. Macrophage changes also occur with ovarian aging, with a unique population of multinucleated macrophage giant cells noted in aging mouse ovaries that were not seen in younger mice [37]. Inflammaging refers to aging-related chronic inflammation, which has been demonstrated in mouse ovaries with corresponding increases in immune-related genes and immune cell populations [45, 46]. Consistent with these age-related changes, we noted an increase in immune response pathways in older (Control PT) versus younger (Control OT) control mice. Notably,

the changes observed in the Post-T ovarian stroma cannot be attributed solely to aging, as the immune response pathway enrichment and increased intensity of macrophage marker staining were found for Post-T mice when directly compared to their corresponding age-matched controls (Control PT).

Some similar ovarian stromal changes have been previously noted in DHT-treated mice, used as a model for polycystic ovary syndrome [26, 27]. Stromal cells from DHT-treated mice have been shown to stain positive for adipocyte differentiation-related protein [27], a marker of lipid droplets, and potentially consistent with a lipid-laden macrophage phenotype. Importantly, both studies in DHT-treated mice mentioned resolution of these stromal changes, suggesting that this may be a transient state. Candelaria et al. reported resolution of stromal changes with superovulation and Sun et al. reported resolution 30 days after DHT capsule removal [26, 27].

In summary, we utilized a mouse model mimicking transmasculine T therapy to characterize ovarian dynamics on T and after T cessation, noting a lack of estrous cyclicity during T therapy, which then resumed as T slowly washed out. Corpora lutea were absent in ovaries On T and reduced Post-T with otherwise comparable follicular distributions. Unexpectedly, we found ovarian stromal aberrations with clusters of large round cells Post-T, which correlated with increased macrophage-associated staining and immune pathway upregulation. T exposure for 6 weeks (On T group) alone did not lead to this stromal phenotype. Based on our prior work, T cessation following implant removal after 6 weeks of T exposure also did not lead to this stromal phenotype [19]. Due to the technical limitations of our injection-based study design, we cannot separate out whether it is the additional exposure to T during the long washout period or the removal of T after a long exposure and resumption of cycling that led to these stromal aberrations. Future studies using long duration T implants could precisely match overall T exposure to determine if a long T duration alone can lead to these stromal changes, or if T cessation and resumption of cyclicity after a long T duration are needed for this stromal immune response. The functional impact of these stromal aberrations has not yet been determined and given similar reports in studies using DHT-treated mice, they may represent a transient state, possibly reversible with more time or with gonadotropin stimulation.

We speculate that the longer duration of T exposure in this study increased the stromal immune response, which may have a suppressive role on corpora lutea formation. Of note, the two mice with corpora lutea present were the earliest mice to resume cycling. We further speculate that the ovarian stromal immune response is reversible. If reversal is possible through processes such as increased time off T or gonadotropin stimulation, this could potentially improve corpora lutea formation to better support a developing pregnancy. Future studies involving a murine breeding comparison after multiple durations of T therapy and T cessation, with and without added gonadotropin stimulation, can assess the functional impact and possible reversibility of these T-induced ovarian changes. If future research reveals that some transmasculine individuals are found to experience difficulty conceiving after a long T duration, further study of their corpora lutea formation and ovarian stromal changes may be warranted.

Conflict of interest

The authors have declared that no conflict of interest exists.

Authors' contributions

H.M.K. designed the study, acquired and analyzed the data, and drafted the article. P.H.H. contributed to the study design, data acquisition, and article review. C.D.C. assisted with histological analyses and article review. F.L.C. assisted with RNA-sequencing and article review. G.R. and L.N. assisted with histological analyses and article review. V.R.E. and A.J. assisted with RNA-sequencing study design and article review. M.A.B. assisted with murine sample collection and article review. D.F.H. and J.Z.L. assisted with RNA-sequencing data analysis and article review. V.P. and M.B.M. contributed to overall study design, data interpretation, and article review. A.S. directed the study and contributed to overall study design, data interpretation, and article review.

Data availability

Original data generated or analyzed during this study are included in this published article or in NCBI's Gene Expression Omnibus (accession number GSE200502, https://www.ncbi.nlm.nih.gov/geo/query/acc.cgi?acc=GSE200502), previously included in part in two published abstracts [47, 48].

Acknowledgment

The authors thank the University of Michigan Advanced Genomics Core and University of Michigan Bioinformatics Core for their support with RNA-sequencing and initial data processing and the University of Virginia Center for Research in Reproduction Ligand Assay and Analysis Core for their support with hormone analyses.

References

1. Hembree WC, Cohen-Kettenis PT, Gooren L, Hannema SE, Meyer WJ, Murad MH, Rosenthal SM, Safer JD, Tangpricha V, T'Sjoen GG. Endocrine treatment of gender-dysphoric/gender-incongruent persons: an Endocrine Society∗ clinical practice guideline. *J Clin Endocrinol Metab* 2017; **102**:3869–3903.
2. Coleman E, Bockting W, Botzer M, Cohen-Kettenis P, DeCuypere G, Feldman J, Fraser L, Green J, Knudson G, Meyer WJ, Monstrey S, Adler RK, *et al*. Standards of care for the health of transsexual, transgender, and gender-nonconforming people, version 7. *Int J Transgenderism* 2011; **13**:165–232.
3. Ethics Committee of the American Society for reproductive medicine. Access to fertility services by transgender persons: an ethics committee opinion. *Fertil Steril* 2015; **104**:1111–1115.
4. Light AD, Obedin-Maliver J, Sevelius JM, Kerns JL. Transgender men who experienced pregnancy after female-to-male gender transitioning. *Obstet Gynecol* 2014; **124**:1120–1127.
5. Ellis SA, Wojnar DM, Pettinato M. Conception, pregnancy, and birth experiences of male and gender variant gestational parents: it's how we could have a family. *J Midwifery Women's Heal* 2015; **60**:62–69.
6. Broughton D, Omurtag K. Care of the transgender or gender-nonconforming patient undergoing in vitro fertilization. *Int J Transgenderism* 2017; **18**:372–375.
7. Light A, Wang LF, Zeymo A, Gomez-Lobo V. Family planning and contraception use in transgender men. *Contraception* 2018; **98**:266–269.

8. Leung A, Sakkas D, Pang S, Thornton K, Resetkova N. Assisted reproductive technology outcomes in female-to-male transgender patients compared with cisgender patients: a new frontier in reproductive medicine. *Fertil Steril* 2019; **112**:858–865.
9. Adeleye AJ, Cedars MI, Smith J, Mok-Lin E. Ovarian stimulation for fertility preservation or family building in a cohort of transgender men. *J Assist Reprod Genet* 2019; **36**:2155–2161.
10. Moseson H, Fix L, Hastings J, Stoeffler A, Lunn MR, Flentje A, Lubensky ME, Capriotti MR, Ragosta S, Forsberg H, Obedin-Maliver J. Pregnancy intentions and outcomes among transgender, nonbinary, and gender-expansive people assigned female or intersex at birth in the United States: results from a national, quantitative survey. *Int J Transgender Heal* 2021; **22**: 30–41.
11. Falck F, Frisén L, Dhejne C, Armuand G. Undergoing pregnancy and childbirth as trans masculine in Sweden: experiencing and dealing with structural discrimination, gender norms and microaggressions in antenatal care, delivery and gender clinics. *Int J Transgender Heal* 2020; **22**:42–53.
12. Amir H, Yaish I, Samara N, Hasson J, Groutz A, Azem F. Ovarian stimulation outcomes among transgender men compared with fertile cisgender women. *J Assist Reprod Genet* 2020; **37**: 2463–2472.
13. Greenwald P, Dubois B, Lekovich J, Pang JH, Safer J. Successful in vitro fertilization in a cisgender female carrier using oocytes retrieved from a transgender man maintained on testosterone. *AACE Clin Case Reports* 2021; **8**:19–21.
14. Esparza LA, Terasaka T, Lawson MA, Kauffman AS. Androgen suppresses in vivo and in vitro LH pulse secretion and neural Kiss1 and Tac2 gene expression in female mice. *Endocrinology* 2020; **161**:1–16.
15. Moravek MB, Kinnear HM, George J, Batchelor J, Shikanov A, Padmanabhan V, Randolph JF. Impact of exogenous testosterone on reproduction in transgender men. *Endocrinology* 2020; **161**: 1–13.
16. De Roo C, Lierman S, Tilleman K, Peynshaert K, Braeckmans K, Caanen M, Lambalk CB, Weyers S, T'Sjoen G, Cornelissen R, De Sutter P. Ovarian tissue cryopreservation in female-to-male transgender people: insights into ovarian histology and physiology after prolonged androgen treatment. *Reprod Biomed Online* 2017; **34**:557–566.
17. Kinnear HM, Constance ES, David A, Marsh EE, Padmanabhan V, Shikanov A, Moravek MB. A mouse model to investigate the impact of testosterone therapy on reproduction in transgender men. *Hum Reprod* 2019; **34**:2009–2017.
18. Bartels CB, Uliasz TF, Lestz L, Mehlmann LM. Short-term testosterone use in female mice does not impair fertilizability of eggs: implications for the fertility care of transgender males. *Hum Reprod* 2020; 1–10.
19. Kinnear HM, Hashim PH, Dela Cruz C, Rubenstein G, Chang FL, Nimmagadda L, Brunette MA, Padmanabhan V, Shikanov A, Moravek MB. Reversibility of testosterone-induced acyclicity after testosterone cessation in a transgender mouse model. *F&S Sci* 2021; **2**:116–123.
20. Futterweit W, Deligdisch L. Histopathological effects of exogenously administered testosterone in 19 female to male transsexuals. *J Clin Endocrinol Metab* 1986; **62**:16–21.
21. Spinder T, Spijkstra JJ, van den Tweel JG, Burger CW, van Kessel H, Hompes PGA, Gooren LJG. The effects of long term testosterone administration on pulsatile luteinizing hormone secretion and on ovarian histology in eugonadal female to male transsexual subjects. *J Clin Endocrinol Metab* 1989; **69**:151–157.
22. Pache TD, Chadha S, Gooren LJG, Hop WCJ, Jaarsma KW, Dommerholt HBR, Fauser BCJM. Ovarian morphology in long-term androgen-treated female to male transsexuals. A human model for the study of polycystic ovarian syndrome? *Histopathology* 1991; **19**:445–452.
23. Ikeda K, Baba T, Noguchi H, Nagasawa K, Endo T, Kiya T, Saito T. Excessive androgen exposure in female-to-male transsexual persons of reproductive age induces hyperplasia of the ovarian cortex and stroma but not polycystic ovary morphology. *Hum Reprod* 2013; **28**:453–461.
24. Grynberg M, Fanchin R, Dubost G, Colau JC, Brémont-Weil C, Frydman R, Ayoubi J-M. Histology of genital tract and breast tissue after long-term testosterone administration in a female-to-male transsexual population. *Reprod Biomed Online* 2010; **20**: 553–558.
25. Hughesdon PE. Morphology and morphogenesis of the Stein-Leventhal ovary and of so-called "Hyperthecosis". *Obstet Gynecol Surv* 1982; **37**:59–77.
26. Candelaria NR, Padmanabhan A, Stossi F, Ljungberg MC, Shelly KE, Pew BK, Solis M, Rossano AM, McAllister JM, Wu S, Richards JS. VCAM1 is induced in ovarian theca and stromal cells in a mouse model of androgen excess. *Endocrinology* 2019; **160**:1377–1393.
27. Sun L-F, Yang Y-L, Xiao T-X, Li M-X, Zhang JV. Removal of DHT can relieve polycystic ovarian but not metabolic abnormalities in DHT-induced hyperandrogenism in mice. *Reprod Fertil Dev* 2019; **31**:1597–1606.
28. Kinnear HM, Tomaszewski CE, Chang FL, Moravek MB, Xu M, Padmanabhan V, Shikanov A. The ovarian stroma as a new frontier. *Reproduction* 2020; **160**:R25–R39.
29. Hashim PH, Kinnear HM, Dela CC, Padmanabhan V, Moravek MB, Shikanov A. Pharmacokinetic comparison of three delivery systems for subcutaneous testosterone administration in female mice. *Gen Comp Endocrinol* 2022; **327**:114090.
30. Martin M. Cutadapt removes adapter sequences from high-throughput sequencing reads. *EMBnetJournal* 2011; **17**:10–12.
31. Andrews S.. *FastQC: A Quality Control Tool for High Throughput Sequence Data*. 2010. http://www.bioinformatics.babraham.ac.uk/projects/fastqc/.
32. Wingett SW, Andrews S. FastQ screen: a tool for multi-genome mapping and quality control. *F1000Research* 2018; **7**:1338.
33. Dobin A, Davis CA, Schlesinger F, Drenkow J, Zaleski C, Jha S, Batut P, Chaisson M, Gingeras TR. STAR: ultrafast universal RNA-seq aligner. *Bioinformatics* 2013; **29**:15–21.
34. Li B, Dewey CN. RSEM: accurate transcript quantification from RNA-Seq data with or without a reference genome. *BMC Bioinform* 2011; **12**:323.
35. Love MI, Huber W, Anders S. Moderated estimation of fold change and dispersion for RNA-seq data with DESeq2. *Genome Biol* 2014; **15**:550.
36. Kim JH, Karnovsky A, Mahavisno V, Weymouth T, Pande M, Dolinoy DC, Rozek LS, Sartor MA. LRpath analysis reveals common pathways dysregulated via DNA methylation across cancer types. *BMC Genom* 2012; **13**:526.
37. Briley SM, Jasti S, McCracken JM, Hornick JE, Fegley B, Pritchard MT, Duncan FE. Reproductive age-associated fibrosis in the stroma of the mammalian ovary. *Reproduction* 2016; **152**: 245–260.
38. Chistiakov DA, Killingsworth MC, Myasoedova VA, Orekhov AN, Bobryshev YV. CD68/macrosialin: not just a histochemical marker. *Lab Invest* 2017; **97**:4–13.
39. Carlock C, Wu J, Zhou C, Ross A, Adams H, Lou Y. Ovarian phagocyte subsets and their distinct tissue distribution patterns. *Reproduction* 2013; **146**:491–500.
40. Wu R, Van der Hoek KH, Ryan NK, Norman RJ, Robker RL. Macrophage contributions to ovarian function. *Hum Reprod Update* 2004; **10**:119–133.
41. Norman RJ, Brannstrom M. White cells and the ovary—Incidental invaders or essential effectors? *J Endocrinol* 1994; **140**: 333–336.
42. Turner EC, Hughes J, Wilson H, Clay M, Mylonas KJ, Kipari T, Duncan WC, Fraser HM. Conditional ablation of macrophages disrupts ovarian vasculature. *Reproduction* 2011; **141**: 821–831.
43. Care AS, Diener KR, Jasper MJ, Brown HM, Ingman WV, Robertson SA. Macrophages regulate corpus luteum development during embryo implantation in mice. *J Clin Invest* 2013; **123**:3472–3487.

44. Pepe G, Locati M, Della Torre S, Mornata F, Cignarella A, Maggi A, Vegeto E. The estrogen-macrophage interplay in the homeostasis of the female reproductive tract. *Hum Reprod Update* 2018; **24**: 652–672.
45. Zhang Z, Schlamp F, Huang L, Clark H, Brayboy L. Inflammaging is associated with shifted macrophage ontogeny and polarization in the aging mouse ovary. *Reproduction* 2020; **159**:325–337.
46. Lliberos C, Liew SH, Zareie P, La Gruta NL, Mansell A, Hutt K. Evaluation of inflammation and follicle depletion during ovarian ageing in mice. *Sci Rep* 2021; **11**:278.
47. Hashim PH, Kinnear HM, Rubenstein GE, Chang FL, Nimmagadda L, Brunette MA, Padmanabhan V, Shikanov A, Moravek MB. Reversibility of hormonal and cyclic disruptions in a transgender mouse model after cessation of testosterone therapy. *Fertil Steril* 2020; **114**:e198.
48. Kinnear HM, Hashim PH, Rubenstein G, Brunette MA, Padmanabhan V, Shikanov A, Moravek MB. Duration of testosterone-induced acyclicity influences corpora lutea formation and stromal changes in a transgender mouse model. *J Endocr Soc* 2020; **4**:A783.